JOURNAL OF AIRCRAFT
Vol. 34, No. 4, July–August 1997

Control of High-Incidence Vortical Flow on Double-Delta Wings Undergoing Sideslip

Sheshagiri K. Hebbar,* Max F. Platzer,† and Wen-Huan Chang‡
U.S. Naval Postgraduate School, Monterey, California 93943-5106

An experimental study of the vortical flow over a baseline double-delta wing model and a diamond-fillet double-delta wing model, both with sharp leading edges, was conducted in a water tunnel using the dye-injection technique at a nominal flow Reynolds number of 1.875×10^4. The diamond fillets at the strake/wing junction increased the wing area of the baseline model by 1%. The main focus of this study was to evaluate the effect of juncture fillets on the vortex core trajectory and the vortex burst location at high angles of attack with sideslip angle. Comparison of the test results between the baseline and the diamond-fillet models indicates a clear delay for the latter model in terms of both the vortex core trajectory, and the breakdown location at high angle of attack, with sideslip angles. The vortex breakdown data for the diamond-fillet model implies lift augmentation during sideslip motion, thus supporting the concept of flow control using fillets. From the maneuvering viewpoint, the data suggest that the diamond-fillet model has a better operational envelope.

Nomenclature

C	=	wing centerline chord
Re	=	freestream Reynolds number, $\rho_\infty U_\infty C/\mu_\infty$
U_∞	=	freestream velocity
X_b	=	streamwise strake vortex burst location
X, Y, Z	=	wing fixed, rectangular coordinates of any point on vortex core trajectory, with X measured streamwise along the wing centerline from the apex, Y measured spanwise outboard from the centerline, and Z measured perpendicular to and away from the wing upper surface
α	=	angle of attack, deg
β	=	angle of sideslip, deg
μ_∞	=	dynamic viscosity of water
ρ_∞	=	density of water

Introduction

AIRCRAFT maneuverability plays a key role in the successful mission accomplishment of a combat aircraft, and therefore, the design of future combat aircraft will have to incorporate features providing enhanced fighter maneuverability during high angle-of-attack (AOA) flight. However, the high AOA flight is limited by the vortex breakdown phenomenon and the onset of vortex asymmetry. As a result, large undesired forces and moments can occur that may lead to departure from controlled flight, and therefore, attention has to be paid to high-rate pitch-up problems, lateral and directional instability problems, and roll and yaw control problems. The strakes and swept wing surfaces have a strong influence on vortex developments and on lateral and directional stability. In fact, experimental studies and flight tests on a variety of aircraft have shown that significant increases in maximum lift and reduction in drag at high lift can be obtained by careful generation and control of concentrated vortices that favorably interact with the flow over a moderate aspect ratio main wing surface.[1]

As the lift at high AOAs is essentially dominated by the vortical flowfield, a good understanding of the basic phenomenon of vortex-dominated flows, the ability to predict such flows, and control them through vortex manipulation, are crucial to enhance aircraft maneuverability. The use of dynamic lift and dynamic flow control by vortex manipulation has now been recognized as an attractive possibility to enhance modern aircraft maneuverability. This control concept relies on modifying the vortex at its point of origin near the shedding point (such as the junction of the strake and wing of a double-delta wing). Both pneumatic and mechanical devices have been investigated as candidates for vortex manipulation. A brief review of vortex control concepts appears in Ref. 2, and reviews of vortex flow control through geometry modification appear in Refs. 3–5.

The numerical study by Kern[2] on vortex flow control through small geometry modifications (fillets) at the strake/wing junction of a double-delta wing suggested that the use of diamond-shaped fillets could enhance the lift by 13.6% at low AOA, and 17.9% at high AOA with a slight improvement in lift-to-drag ratio. It even suggested that the fillets may be good candidates for roll control devices. Note that the fillets are envisioned as being deployable on demand at the junction of the strake and the wing during air combat maneuver or carrier landing approach. A symmetrical deployment of the fillets would result in enhanced lift and longitudinal control, whereas an asymmetric deployment would provide lateral–directional control. The experimental investigation of Hebbar et al.[6] has verified the concept of flow control using fillets, during both nonmaneuver (static pitch) and maneuver (dynamic pitch) conditions.

Maneuvers at high AOA and appreciable sideslip angles provide more agility, and are therefore desirable. Wind-tunnel investigations of double-delta wings reported in Refs. 7–9, and water-tunnel investigations in Refs. 6, 10, and 11 have generally focused attention on pitching conditions of the model (with zero sideslip). Wind-tunnel investigations of vortex flow characteristics are reported in Refs. 12 and 13 for sideslipping, simple-delta wings, and in Ref. 14 for a strake–wing configured fighter model. Water-tunnel flow visualization results of slender wing leading-edge vortex flow characteristics up to

Presented as Paper 96-0663 at the AIAA 34th Aerospace Sciences Meeting, Reno, NV, Jan. 15–19, 1996; received Dec. 15, 1996; revision received April 1, 1997; accepted for publication April 2, 1997.

*Adjunct Professor, Department of Aeronautics and Astronautics. Associate Fellow AIAA.

†Professor, Department of Aeronautics and Astronautics. Associate Fellow AIAA.

‡Graduate Student, Department of Aeronautics and Astronautics; currently Lt. Col., Republic of China Air Force. Member AIAA.

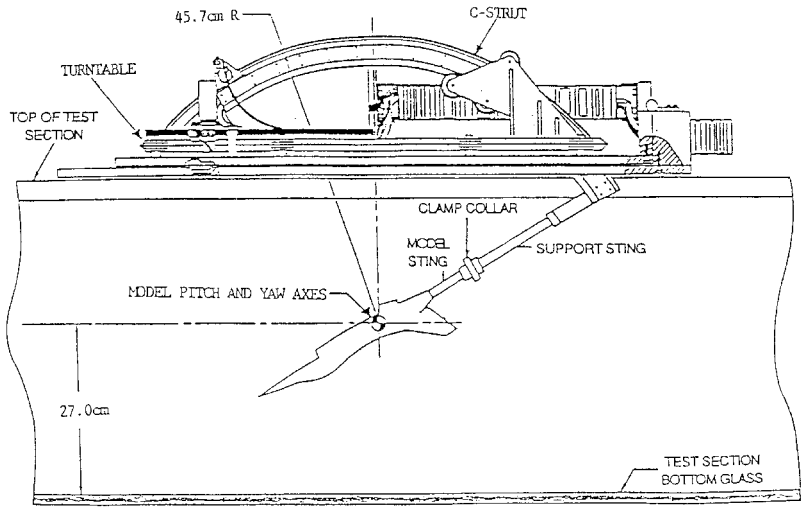

Fig. 1 Model support system of the NPS water tunnel.

high AOAs and sideslip are reported in Ref. 1, and they show similar trends with sideslip when compared with the results from Ref. 15. A recent low-speed wind-tunnel investigation[16] deals with the effects of sideslip on double-delta wings. Reference 17 discusses the results of a water-tunnel flow visualization study on a sideslipping, canard-configured, X-31A-like fighter model. In general, a large body of data exists on high-incidence vortical flows, but the data on double-delta wings undergoing sideslip at high AOA is rather limited.

More experimental studies are needed to investigate the resulting vortex structure on double-delta wings and to establish whether small deployable fillets could provide substantial control over the vortex core trajectory and bursting at high AOA during maneuvering conditions with sideslip. To this end, an experimental program was conducted in the Naval Postgraduate School (NPS) water tunnel to visualize vortical flows on a sharp-edged, 76/40-deg cropped, double-delta wing baseline model, and its derivative with a small geometry modification (in the form of a diamond-shaped fillet) at the junction of the strake and wing leading edges. Extensive, dye-injection flow visualization methods were utilized to track vortex trajectories and vortex bursting for a range of model AOA and sideslip. The results presented in this paper should be of interest to researchers working on similar configurations, especially in view of the streamlined support system used. Additional details of the investigations appear in Refs. 18 and 19.

Experiment

Water-Tunnel Facility

The NPS water tunnel is a closed-circuit facility for studying a wide range of aerodynamic and fluid dynamic phenomena (see Fig. 1 of Ref. 6). Its key design features are high flow quality, horizontal orientation, and continuous operation. The test section is 38 cm wide, 51 cm high, and 152 cm long. Water velocities of up to 30.5 cm/s with a turbulence intensity of <1% are possible in the test section. The dye supply system for injecting color dyes consists of six pressurized color dyes using water-soluble food coloring, and is provided with individually routed lines from the dye reservoir to the model support system attached to the top of the tunnel (Fig. 1). The model is usually mounted upside down in the test section. The model support system utilizes a C-strut to vary the pitch travel up to 50 deg between the limits of −10 and 110 deg, and a turntable to provide yaw variations up to ±20 deg. The two servomotors of the model attitude control system provide independent control of model pitch and yaw with two rates.

Double-Delta Wing Models

The baseline double-delta wing model and the diamond-fillet double-dealt wing model used in this investigation are shown

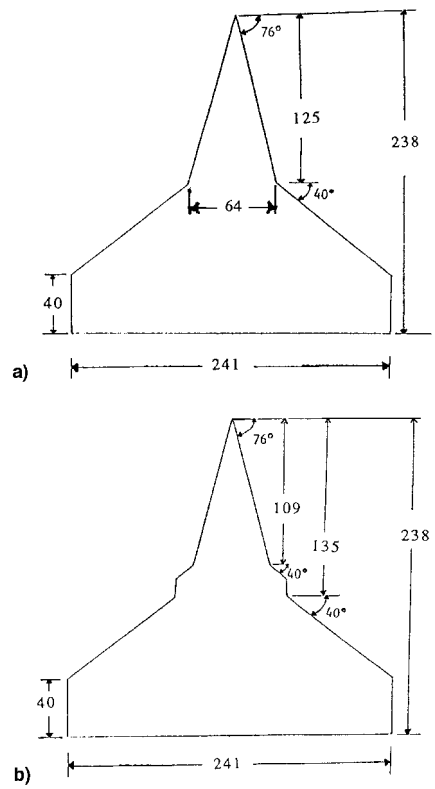

Fig. 2 Double-delta wing models: a) baseline model (no fillet) and b) diamond-fillet model. All dimensions are in millimeters.

in Fig. 2. The models were constructed of 6.3-mm-thick Plexiglas® with a 76-deg sweep for the strake and a 40-deg sweep for the wing, both with sharp, beveled leading edges and flat top surfaces. Each model has a chord C of 238 mm, a span of 241 mm, and an aspect ratio of 2.34. The geometry modification (fillet) at the intersection (junction or kink) of the strake and wing leading edges increased the planform area of the baseline model by 1%. The models were used in the previous investigation[6] and their dimensions are identical to the ones used by Kern.[2] The upper surface of the models had grid lines marked for easy identification of vortex core trajectory and burst location. The location of the dye-tube tip and the rate of dye-injection were crucial to obtain a good flow visualization of the vortical flowfield. Satisfactory dye injection for vortex visualization purposes was achieved by positioning small brass tubes flat on the model bottom surface with their tips very

close to the vortex shedding points (e.g., apex, kink, fillet), and adjusting the injection rate properly.

Experimental Program and Test Conditions

The experimental program consisted of the flow visualization of vortex trajectory and breakdown on the upper surface of the models, using the dye-injection technique for several AOAs with and without sideslip. The AOA varied from 10 to 50 deg, and the angle of sideslip (AOS) varied from 0 to 15 deg, both in 5-deg increments. The U_∞ in the tunnel was maintained at a nominal value of 7.6 cm/s, corresponding to a nominal Re of 1.875×10^4, based on the centerline chord. Both still-picture photography and videotape recordings were used for documentation of dye-flow visualization of the models in both topview and sideview.

Results and Discussion

The trajectories of the strake and wing vortices were easily recognized during the flow visualization study as the dye fluid issuing out of the apex and kink locations exhibited features characteristic of a vortex core trajectory.[6] Being a coherent vortex, the strake vortex core was easier to identify. Water-tunnel flow visualization studies of double-delta wing models reported by Thompson[10] clearly confirm the presence of the wing vortex for $Re \geq 1.5 \times 10^4$. As the Reynolds number in the present study exceeded this value, it reinforces the direct, visual interpretation of the dyeline originating at the kink as representing a vortex core. In the following discussion the kink vortex of the baseline/fillet model is referred to as the wing vortex/fillet vortex, respectively.

During this study, both the windward side and leeward side data were collected for analysis. Data reduction essentially consisted of measuring the vortex core locations along the model centerline from the apex (X coordinate) and outboard from the model centerline (Y coordinate), and the burst location X_b of the vortices shed off the leading edge of the model. The vortex core trajectories were constructed by plotting the Y coordinate vs the X coordinate at each AOA for different sideslip angles, and the burst location plots were constructed by plotting the burst location X_b vs AOA for different sideslip angles. Note that the end of the core in the trajectory plots signifies the vortex burst location.

The vortex core locations and the burst locations were visually selected from the videotape/photographs in a careful, consistent manner, and then nondimensionalized using the centerline chord length. Nevertheless, there will be some inaccuracies in the data because of the difficulty in assessing core location and burst point associated with unsteady vortex bursting, particularly at high AOAs. In fact, during the experiments, the vortex burst location at any AOA fluctuated up to ± 19 mm (about $\pm 0.08C$); therefore, the reported values should be viewed as mean values. In addition, it was extremely difficult to assess core locations of wing and fillet vortices when the AOA was higher than 30 deg, and so there is no data for the wing and fillet vortices above 30 deg. The data on vortex trajectory and breakdown are tabulated in Ref. 18.

In the following sections, the behavior of the vortical flow and the effect of fillets are described, with emphasis on strake vortex core trajectories and vortex bursting at high AOA with sideslip.

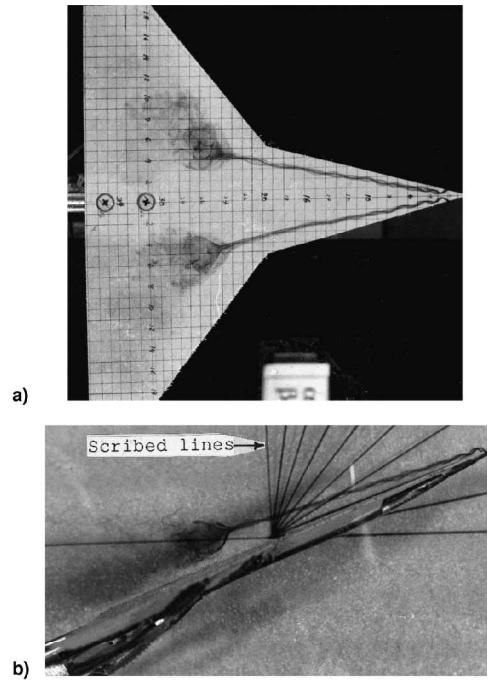

Fig. 3 Strake vortex core trajectories for the baseline model at AOA = 20 deg and AOS = 0 deg (flow from right to left): a) plan view and b) side view.

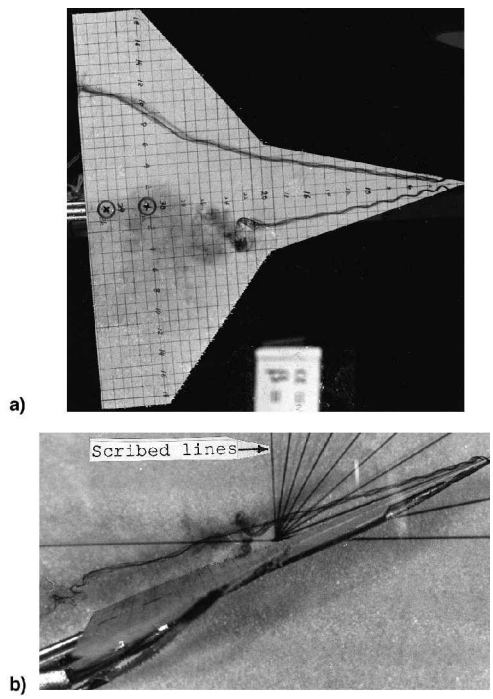

Fig. 4 Strake vortex core trajectories for the baseline model at AOA = 20 deg and AOS = 5 deg (flow from right to left): a) plan view and b) side view.

Visualization of Vortical Flowfield

Figures 3 and 4 are typical flow visualization photographs showing the strake vortex core on the baseline model at AOA = 20 deg and AOS = 0 and 5 deg, respectively. Note that the nonvisualization of the wing vortices was deliberate and intended to facilitate identification of strake vortex core/burst location. In the absence of sideslip, the vortical flowfield develops symmetrically over the upper surface of the model as the AOA is increased from 0 deg. At 10-deg AOA, the strake vortex core is already well developed and is seen to burst just around the trailing edge.[18] With a further increase in AOA, the vortex core lengths shorten, the burst locations move upstream (see Fig. 3), and finally approach the apex. In the presence of sideslip, the vortical flowfield becomes asymmetric over the upper surface of the model, leading to asymmetric vortex burst locations. Figure 4 highlights the large effect of a small sideslip angle ($\beta = 5$ deg) on the burst locations at AOA = 20 deg, namely, the forward movement of the burst location on the windward side and the rearward movement on the leeward

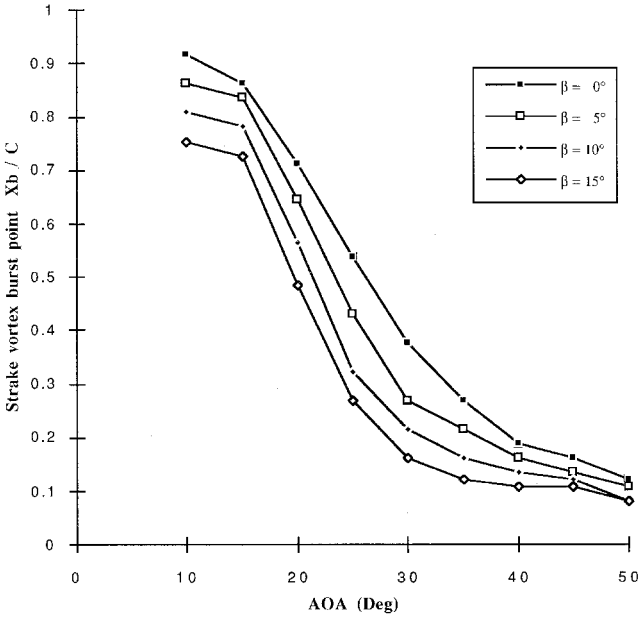

Fig. 5 Strake vortex burst point data for the baseline model (windward side).

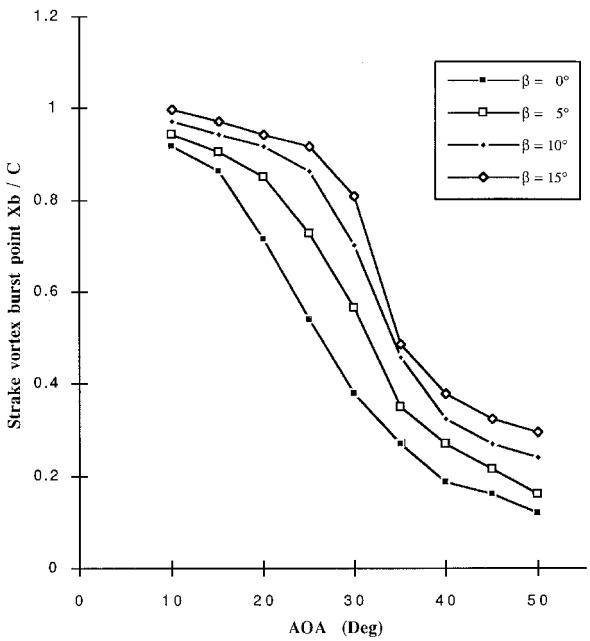

Fig. 6 Strake vortex burst point data for the baseline model (leeward side).

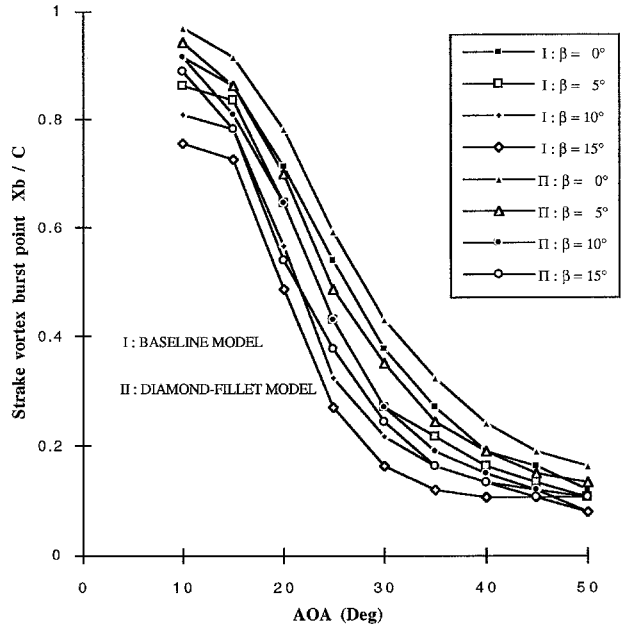

Fig. 7 Comparison of strake vortex burst point data for two models (windward side).

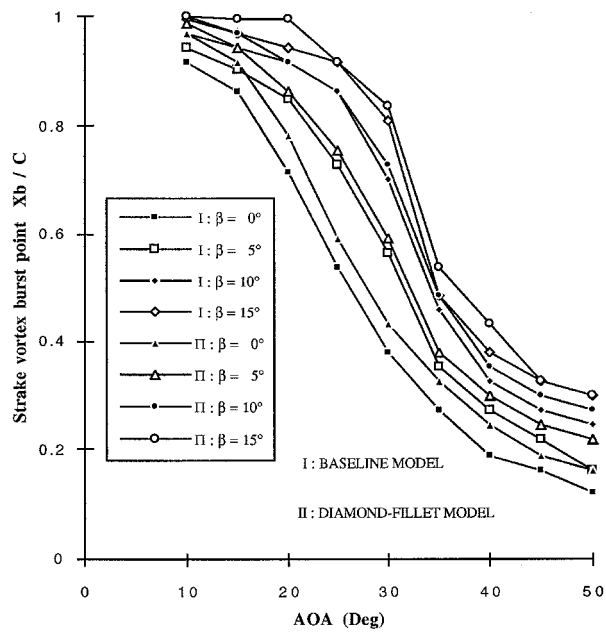

Fig. 8 Comparison of strake vortex burst point data for two models (leeward side).

side. Note the relatively greater sideslip effect on the leeward side.

Effect of AOA on Vortex Core Breakdown at Zero Sideslip

The strake vortex core burst location for the baseline model as a function of AOA at different sideslip angles is shown for the windward and leeward sides in Figs. 5 and 6, respectively. Note that for the zero sideslip case, there is no difference between the windward and leeward sides, and the plots corresponding to $\beta = 0$ deg in these figures are identical. The plots show that the longitudinal location of vortex breakdown at 10-deg AOA for the symmetric condition ($\beta = 0$ deg) occurs at $0.92C$ from the apex. The strake vortex burst point moves upstream as AOA increases, and moves to $0.12C$ at 50-deg AOA. The slope of the curve is steep in the 15 deg < AOA < 30 deg range, implying faster upstream movement of the burst in this range. These findings are in good agreement with those of earlier investigations.[6–11] Similar trends are noticed in the case of wing vortex burst location plots, but the slopes imply small upstream movements of burst locations.[18]

The strake–vortex and fillet–vortex burst location plots for the diamond-fillet model exhibit AOA-dependent burst movement features that are qualitatively similar to those for the baseline model described earlier. A comparison of the strake vortex burst location data for the baseline and diamond-fillet models on the windward and leeward sides is shown in Figs. 7 and 8, respectively. For the zero sideslip case ($\beta = 0$ deg), the slopes of the curves are pretty much the same, but the burst locations for the diamond-fillet model lag those for the baseline model throughout the AOA range tested by about 8%. These plots therefore imply a burst delay for the diamond-fillet model.

Effect of AOS on Vortex Core Breakdown

Figures 5 and 6 highlight the effect of sideslip on strake vortex core burst locations. These plots clearly demonstrate the differential effect of small sideslip angles on the burst location at any given AOA; namely, the forward (upstream) movement of the burst location on the windward side and the rearward (downstream) movement on the leeward side. Large burst movements are observed in the 20 deg < AOA < 35 deg range on both sides; the leeward side showing relatively greater sideslip effect. Maximum sideslip effect on the burst movement is seen around AOA = 30 deg on both sides. Furthermore, the effect is pronounced at small sideslip angles (β < 10 deg), but is diminished at higher sideslip angles (β > 10 deg). Note that the influence of sideslip angle on burst location can be explained in terms of the effective sweep angle for the windward and leeward sides.[1,17] With sideslip present, the effective sweep angle increases on the leeward side, resulting in a more stable vortex with delayed bursting, but decreases on the windward side, leading to a less stable vortex with early bursting. Similar qualitative trends are also noticed in the case of wing vortex burst location plots.[18] Of particular interest on the leeward side is that for the β = 15 deg case, the burst locations move downstream of the wing trailing edge with an increase of AOA.

The sideslip effects observed on the burst location of the strake and fillet vortices on the windward and leeward sides of the diamond-fillet model are qualitatively similar to those observed on the baseline model described earlier. Figures 7 and 8 compare these effects on the baseline and diamond-fillet models for the windward and leeward sides, respectively. It is clear from the plots, that over the AOA range tested, the major effect of sideslip is to delay the vortex bursting on the leeward side and advance it on the windward side. With few exceptions, the difference in burst point because of changes in AOA between the two models at zero sideslip (β = 0 deg) is preserved for both the leeward and windward sides with increasing sideslip. Note that in comparison to the baseline model, the sideslip effect on the diamond-fillet model is more pronounced on the leeward side, but less pronounced on the windward side. In other words, the presence of the fillet is seen to enhance the sideslip effect on the burst location on the leeward side, but reduce it on the windward side.

Effect of AOA on Vortex Core Trajectory at Zero Sideslip

Typical nondimensional $X-Y$ plots of the strake vortex core trajectories for the windward and leeward sides of the baseline model at different sideslip angles are shown in Figs. 9–11 for AOAs of 10, 20, and 30 deg, respectively. For the zero sideslip case, there is practically no difference between the windward and leeward sides, and the plots corresponding to β = 0 deg in these figures are essentially symmetrical with respect to the centerline chord. They clearly indicate that, as the AOA increases at zero sideslip, the strake vortex core length decreases (the burst location moves upstream), and the vortex core moves inboard toward the centerline chord. Similar trends are observed in the case of wing vortex trajectories at zero sideslip angle. These observations are in general agreement with the earlier wind- and water-tunnel investigations,[7–11] and the recent investigations of Verhaagen et al.[20] and Hebbar et al.[6]

The nondimensional $X-Y$ plots of the strake–vortex core and fillet–vortex core trajectories for the diamond-fillet model at zero sideslip angle exhibit trends that are essentially similar to those for the baseline model described earlier, namely, a

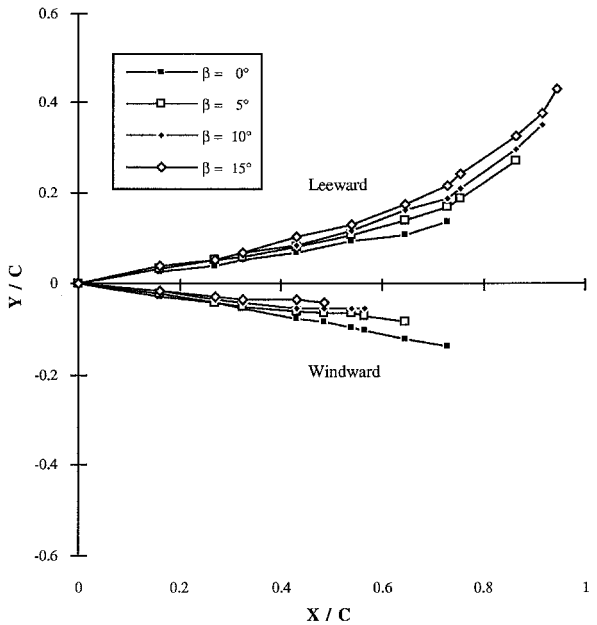

Fig. 10 Strake vortex core trajectory for the baseline model at AOA = 20 deg.

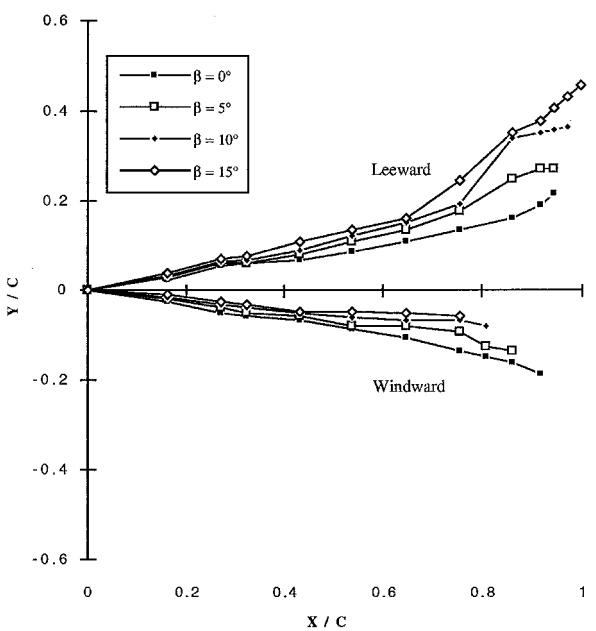

Fig. 9 Strake vortex core trajectory for the baseline model at AOA = 10 deg.

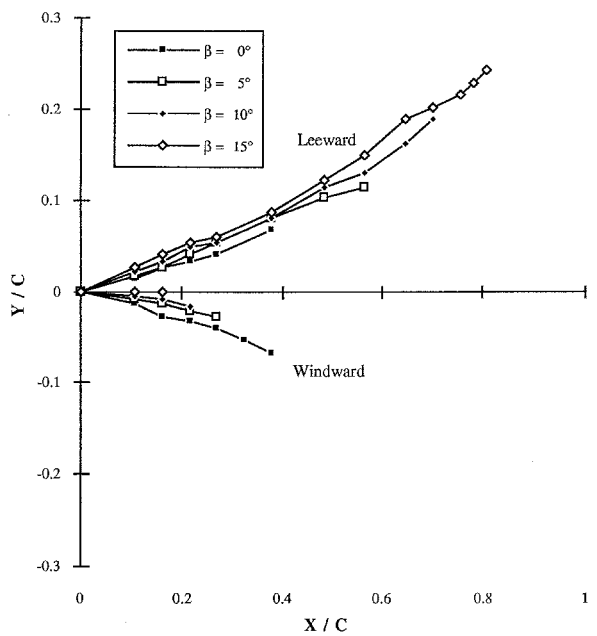

Fig. 11 Strake vortex core trajectory for the baseline model at AOA = 30 deg.

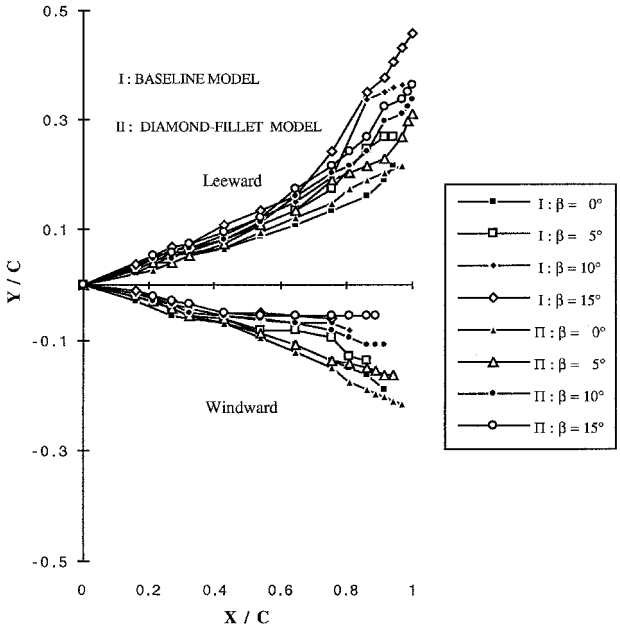

Fig. 12 Comparison of strake vortex core trajectories for two models at AOA = 10 deg.

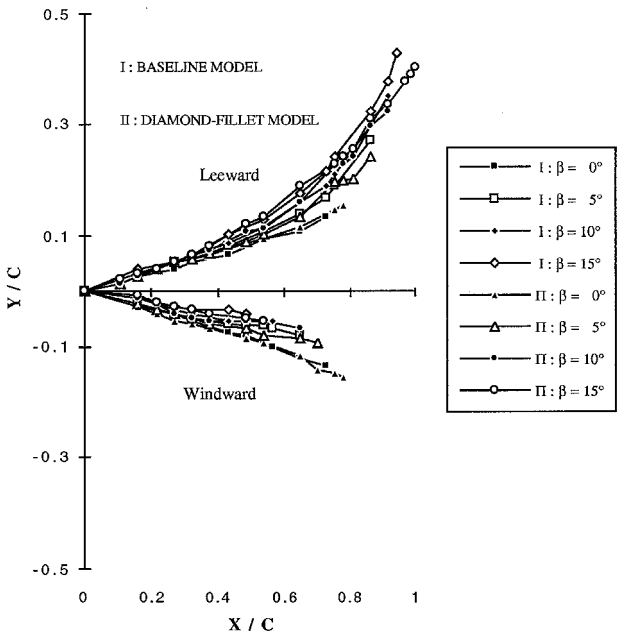

Fig. 13 Comparison of strake vortex core trajectories for two models at AOA = 20 deg.

reduction in core length and inboard movement of the vortex core with an increase of AOA. Figures 12–14 compare the strake vortex trajectory data for the baseline and the diamond-fillet models at different sideslip angles, for AOAs of 10, 20, and 30 deg, respectively. An examination of the plots for the zero sideslip case ($\beta = 0$ deg) indicates that the strake vortex trajectory of the baseline model is closer to the centerline chord at low AOA, but moves outboard with increasing AOA. Moreover, because of the delay in strake vortex breakdown associated with the diamond-fillet model, this core will have a longer length in these figures.[6]

Effect of AOS on the Vortex Core Trajectory

Figures 9–11 highlight the sideslip effect on the strake vortex core trajectories. These plots clearly demonstrate that with increasing sideslip input, at any given AOA, the windward/

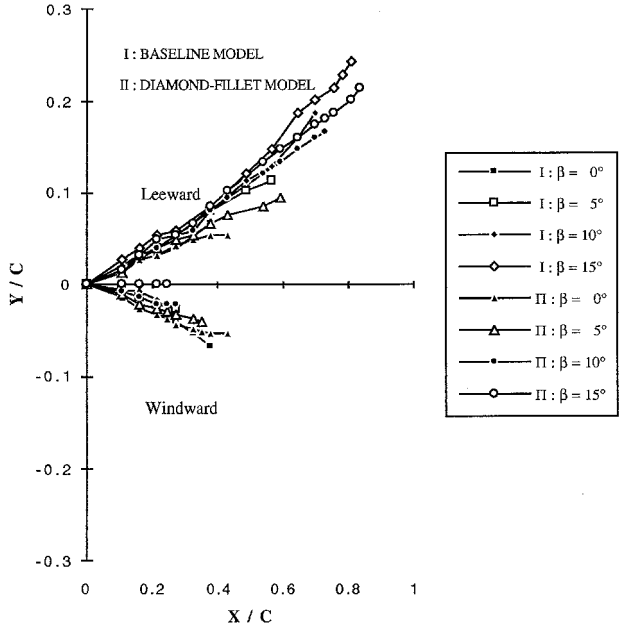

Fig. 14 Comparison of strake vortex core trajectories for two models at AOA = 30 deg.

leeward vortex core length decreases/increases and the trajectory moves inboard/outboard. Note that the core length is a strong, decreasing function of angle of attack, and the degree of asymmetry at any given angle of attack increases with sideslip. Similar qualitative trends are also noticed in the case of wing vortex core trajectories.[18]

The sideslip effects observed on the strake- and fillet-vortex core trajectories on the windward and leeward sides of the diamond-fillet model are qualitatively similar to those observed on the baseline model described earlier. Figures 12–14 compare these effects on the baseline and diamond-fillet models at AOAs of 10, 20, and 30 deg, respectively. These plots show that the vortex core lengths on both the windward and leeward sides of the diamond-fillet model are usually longer than their counterparts for the baseline model. Also, the vortex trajectories on the diamond-fillet model tend to remain further outboard/inboard on the windward side/leeward side. This implies that the fillet is in effect counteracting (delaying) the sideslip effect on vortex trajectory.

The combined sideslip effect of the vortex core asymmetry and vortex breakdown asymmetry may, under certain conditions, cause unstable rolling and yawing moment increments, leading to severe lateral–directional control problems.[1] As the fillets tend to counteract the sideslip effects, they can be used as vortex manipulators to improve the directional stability characteristics at high AOA.

It should be noted here that both the vortex trajectory and the breakdown characteristics are influenced by the phenomenon of vortex interaction, which depends on several parameters, including flow Reynolds number.[6] The results of a recent study[21,22] have shown that the flow Reynolds number will influence the vortical flowfield generated by a double-delta wing, and that the data from water-tunnel studies will reflect more closely the wind-tunnel data as the flow Reynolds number is increased. For the following discussion, it will suffice to note that the results of the current (low Reynolds number) investigation[18,19] suggest that the vortex interaction points on the windward/leeward side move upstream and inboard/downstream and outboard with sideslip.

Comparison of Operational Envelope

The flow visualization data of each model discussed earlier clearly indicate that the burst location is a function of both AOA and AOS. With increasing AOA, the burst location

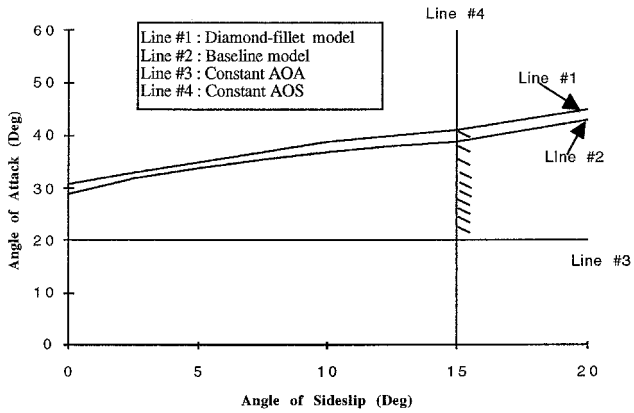

Fig. 15 Comparison of high AOA operational envelope for two models.

moves upstream, implying loss of lift. However, the rate of burst movement is not uniform, being maximum in the 15 deg < AOA < 30 deg range. With sideslip input at any AOA, both the strake vortex core burst location and the vortex interaction point move upstream and inboard on the windward side, but downstream and outboard on the leeward side. These movements yield a vortex trajectory with a shorter core that is closer to the centerline chord on the windward side, but they yield a vortex trajectory with a longer core that is farther from the centerline chord on the leeward side. Assuming these movements have an adverse effect on lift generation, loss of lift increases with sideslip. Further asserting this assumption, at a 15-deg sideslip angle, the lift-loss increases considerably for AOA > 30 deg. Thus, based on the lift-loss consideration, the regime of high AOA with large sideslip angles may not be a favored choice.

However, maneuvers at high AOA and appreciable sideslip angles provide more agility and are therefore desirable. It is advantageous to have vortex flow control in this regime. It is illuminating to see how the diamond-fillet model compares with the baseline model in the maneuver range. To see qualitative trends, the flow visualization data have been utilized to construct for each model an operational envelope for maneuvering.[18] The operational envelopes for the baseline model and the diamond-fillet model are compared in Fig. 15. These are constructed based on the assumption that AOS is limited to 15 deg (for lack of test data at higher angles), minimum operating AOA to 20 deg, and the burst point moves no closer than $0.4C$ from the apex (this assumes that there is still sufficient lift developed to carry out the maneuver and also to avoid uncontrolled pitch-up). It is clearly demonstrated in Fig. 15 that the diamond-fillet model has a better operational envelope.

Thus, the flow visualization data have substantiated qualitatively the concept of flow control by fillets for maneuvering conditions involving sideslip. Force-balance data are certainly needed to completely validate the concept on a quantitative basis and for direct comparison with the numerical prediction.

Conclusions

A flow visualizations study of the vortical flow over a baseline double-delta wing model and a diamond-fillet double-delta wing model, both with sharp leading edges, was conducted in the NPS water tunnel. The main focus of this study was to evaluate the effect of the diamond fillet on the vortex core trajectory and burst location over the wing surface at high AOA with sideslip. The following conclusions are based on the results of the experimental investigation at $Re = 1.875 \times 10^4$.

1) At zero sideslip, the vortex trajectories and burst locations are symmetric over the AOA range tested. With an increase in the AOA, the vortex burst point moves upstream and the vortex core length decreases.

2) Both the vortex core trajectory and the burst location are functions of sideslip angle. At a constant AOA, as the angle of sideslip increases, the windward side strake–vortex trajectory moves inboard with its burst point moving upstream, whereas the leeward-side strake–vortex trajectory moves outboard with its burst point moving downstream.

3) Comparison of the test results between the baseline model and the diamond-fillet model in the high-AOA range tested shows that the delay in strake–vortex trajectory and breakdown associated with the diamond-fillet model is preserved with sideslip. Therefore, the diamond fillets can be viewed as flow controllers and lift augmenters during sideslip motion.

Acknowledgments

This work was supported by the U.S. Naval Air Warfare Center, Aircraft Division, Patuxent River, Maryland. The technical discussions with Steve Kern are acknowledged. The authors thank Ron Ramaker for fabricating the models.

References

[1]Erickson, G. E., "Flow Studies of Slender Wing Vortices," AIAA Paper 80-1423, July 1980.

[2]Kern, S., "Vortex Flow Control Using Fillets on a Double-Delta Wing," *Journal of Aircraft*, Vol. 30, No. 6, 1993, pp. 818–825; also AIAA Paper 92-0411, Jan. 1992.

[3]Lamar, J. E., "Nonlinear Lift Control at High Speed and High Angle of Attack Using Vortex Flow Technology," *Special Course on Fundamentals of Fighter Aircraft Design*, AGARD-R-740, Oct. 1987, pp. 4.1–4.23.

[4]Rao, D. M., "Vortical Flow Management for Improved Configuration Aerodynamics—Recent Experiences," *AGARD Symposium on Aerodynamics of Vortical Type Flows in Three Dimensions*, CP-342, AGARD, Rotterdam, The Netherlands, April 1983 (Paper 30).

[5]Rao, D. M., and Campbell, J. F., "Vortical Flow Management Techniques," *Progress in Aerospace Sciences*, Vol. 24, No. 3, 1987, pp. 173–224.

[6]Hebbar, S. K., Platzer, M. F., and Alkhozam, A. M., "Experimental Study of Vortex Flow Control on Double-Delta Wings Using Fillets," *Journal of Aircraft*, Vol. 33, No. 4, 1996, pp. 743–751; also AIAA Papers 94-0626, Jan. 1994 and 95-0649, Jan. 1995.

[7]Verhaagen, N. G., "An Experimental Investigation of the Vortex Flow over Delta and Double-Delta Wings at Low Speeds," Delft Univ. of Technology, Rept. LR-372, Delft, The Netherlands, Sept. 1983.

[8]Olsen, P., and Nelson, R., "Vortex Interaction over Double-Delta Wings at High Angles of Attack," AIAA Paper 89-2191, July 1989.

[9]Graves, T. V., Nelson, R. C., Schwimley, S. L., and Ely, W. L., "Aerodynamic Performance of Strake Wing Configurations," *High-Angle-of-Attack Technology*, Vol. 1, NASA CP-3149, Pt. 1, May 1992, pp. 173–204.

[10]Thompson, D. H., "A Visualization Study of the Vortex Flow Around Double-Delta Wings," Aeronautical Research Lab., Aerodynamics Rept. 165, Melbourne, Australia, Aug. 1985.

[11]Hebbar, S. K., Platzer, M. F., and Li, F. H., "A Visualization Study of the Vortical Flow over a Double-Delta Wing in Dynamic Motion," AIAA Paper 93-3425, Aug. 1993.

[12]Hummel, D., and Redeker, G., "Ueber den Einfluss des Aufplatzens der Wirbel auf die aerodynamische Beiwerte von Deltafluegeln mit kleinen Seitenverhaeltnes bein Scheibeflug," *Jahrbuch der W.G.L.R.*, 1967, pp. 232–240.

[13]Verhaagen, N. G., and Naarding, S. H. J., "Experimental and Numerical Investigation of Vortex Flow over a Sideslipping Delta Wing," *Journal of Aircraft*, Vol. 26, No. 11, 1989, pp. 971–978.

[14]Hebbar, S. K., and Leedy, D. H., "Wind-Tunnel Investigation of a Fighter Model at High Angles of Attack," *Journal of Aircraft*, Vol. 29, No. 6, 1992, pp. 1091–1097.

[15]Hummel, D., "Investigation of Vortex Bursting on Slender Delta Wings," *Zeitschrift für Flugwissenschaften*, Vol. 13, No. 5, 1965, pp. 158–168.

[16]Grismer, D., and Nelson, R., "The Aerodynamic Effect of Sideslip on Double-Delta Wings," AIAA Paper 93-0053, Jan. 1993.

[17]Hebbar, S. K., Platzer, M. F., and Kim, C. H., "Experimental Investigation of Vortex Breakdown over a Sideslipping Canard-Configured Aircraft Model," *Journal of Aircraft*, Vol. 31, No. 4, 1994, pp. 998–1001.

[18]Chang, W. H., "Effect of Juncture Fillets on Double-Delta Wings Undergoing Sideslip at High Angles of Attack," M.S. Thesis, U.S. Naval Postgraduate School, Monterey, CA, Sept. 1994.

[19]Hebbar, S. K., Platzer, M. F., and Chang, W. H., "Juncture Fillets for Vortex Flow Control on Double-Delta Wings Undergoing Sideslip," AIAA Paper 96-0663, Jan. 1996.

[20]Verhaagen, N. G., Jenkins, L. N., Kern, S. B., and Washburn, A. E., "A Study of the Vortex Flow over a 76/40-deg Double-Delta Wing," AIAA Paper 95-0650, Jan. 1995.

[21]Fritzelas, A. E., Platzer, M. F., and Hebbar, S. K., "Effect of Reynolds Number on High-Incidence Flow over Double-Delta Wings," AIAA Paper 97-0046, Jan. 1997.

[22]Fritzelas, A. E., "A Water Tunnel Investigation of the Influence of Reynolds Number on the High-Incidence Flow over Double-Delta Wings," M.S. Thesis, U.S. Naval Postgraduate School, Monterey, CA, March 1996.